Binuclear Palladium Macrocycles Synthesized via the Weak-Link Approach

Adam H. Eisenberg,[†] Felicia M. Dixon,[†] Chad A. Mirkin,*[,†] Charlotte L. Stern,[†] Christopher D. Incarvito,[‡] and Arnold L. Rheingold[‡]

Department of Chemistry, 2145 Sheridan Road, Northwestern University, Evanston, Illinois 60208, and Department of Chemistry and Biochemistry, University of Delaware, Newark, Delaware 19716

Received December 6, 2000

The "weak-link approach" to metallomacrocycle synthesis has been employed to synthesize a series of Pd(II) macrocycles in high yield. Although this approach has been used to construct several Rh(I) complexes with a variety of ligands, the generality of this methodology with respect to transition metals has not been demonstrated. When added to $[Pd(NCCH_3)_4][BF_4]_2$, the phosphinoalkyl ether or thioether ligands produce "condensed intermediates", $[(\mu\text{-}(1,4\text{-}(PPh_2CH_2CH_2X)_2\text{−}Y)_2Pd_2)][BF_4]_4$ (**4**, X = O, Y = 2,3,5,6-$((CH_3)_4C_6)$; **5**, X = O, Y = C_6H_4; **6**, X = S, Y = C_6H_4), containing strong P−Pd bonds and weaker O−Pd or S−Pd bonds. The weak bonds of these intermediates can be quantitatively broken through simple ligand substitution reactions to generate the macrocyclic structures $[(\mu\text{-}(1,4\text{-}(PPh_2CH_2CH_2X)_2\text{−}Y)_2(Z)_4Pd_2)][BF_4]_n$ (**7**, X = O, Y = 2,3,5,6-$((CH_3)_4C_6)$, Z = CH_3CN, $n = 4$; **8**, X = O, Y = C_6H_4, Z = CH_3CN, $n = 4$; **9**, X = O, Y = 2,3,5,6-$((CH_3)_4C_6)$, Z = CN, $n = 0$; **10**, X = O, Y = C_6H_4, Z = CN, $n = 0$; **11**, X = S, Y = C_6H_4, Z = CN, $n = 0$), in quantitative yields. The extension of this approach to Pd(II) should provide new pathways for modifying the binding and catalytic capabilities of these complexes. Solid-state structures as determined by single-crystal X-ray diffraction studies are presented for compounds **6**, **8**, and **9**.

In recent years, metallomacrocycles have received a significant amount of attention due to their encapsulating properties and potential applications in catalysis, sensing, molecular electronics, and facilitated small molecule transport.[1−3] Several groups employ a variety of strategies, such as the "molecular library" or "symmetry interaction" approaches, to construct metallomacrocycles, and reviews documenting much of this work have appeared in the literature.[4−9] Our group has pioneered a methodology now known as the "weak-link approach" to the synthesis of bimetallic macrocycles from elementary metal and ligand precursors.[10−14] This approach utilizes flexible multidentate ligands, often referred to as hemilable ligands,[15−24] to yield condensed intermediates that contain both strong and weak bonds (Scheme 1 and Scheme 2). The weak bonds in these intermediates can be broken through ligand substitution processes to produce macrocyclic or supramolecular complexes. This strategy circumvents the entropic penalties associated with directly targeting a flexible macrocyclic product and often allows one to prepare the targeted structures in exceptionally high yields.

Typically, ligands that have a rigid aromatic spacer flanked with flexible phosphinoalkyl ether or thioether

* To whom correspondence should be addressed. Fax: (847) 467-5123. E-mail: camirkin@chem.nwu.edu.
[†] Northwestern University.
[‡] University of Delaware.

(1) Lehn, J.-M. *Supramolecular Chemistry*; VCH: New York, 1995.
(2) Vogtle, F. *Supramolecular Chemistry*; Wiley: Chichester, 1991.
(3) Mirkin, C. A.; Ratner, M. A. *Annu. Rev. Phys. Chem.* **1992**, *43*, 719−754.
(4) Slone, R. V.; Benkstein, K. D.; Belanger, S.; Hupp, J. T.; Guzei, I. A.; Rheingold, A. L. *Coord. Chem. Rev.* **1998**, *171*, 221−243.
(5) Caulder, D. L.; Raymond, K. N. *J. Chem. Soc., Dalton Trans.* **1999**, 1185−1200.
(6) Leininger, S.; Olenyuk, B.; Stang, P. J. *Chem. Rev.* **2000**, *100*, 853−908.
(7) Fujita, M. In *Comprehensive Supramolecular Chemistry*; Lehn, J.-M., Ed.; Elsevier Science Ltd: New York, 1996; Vol. 9, pp 253−282.
(8) Holliday, B. J.; Mirkin, C. A. *Angew. Chem.* **2001**, in press.
(9) Swiegers, G. F.; Malefetse, T. J. *Chem Rev.* **2000**, *100*, 3483−3538.
(10) Farrell, J. R.; Mirkin, C. A.; Guzei, I. A.; Liable-Sands, L. M.; Rheingold, A. L. *Angew. Chem., Int. Ed. Engl.* **1998**, *37*, 465−467.
(11) Farrell, J. R.; Mirkin, C. A.; Liable-Sands, L. M.; Rheingold, A. L. *J. Am. Chem. Soc.* **1998**, *120*, 11834−11835.
(12) Holliday, B. J.; Farrell, J. R.; Mirkin, C. A.; Lam, K.-C.; Rheingold, A. L. *J. Am. Chem. Soc.* **1999**, *121*, 6316−6317.
(13) Farrell, J. R.; Eisenberg, A. H.; Mirkin, C. A.; Guzei, I. A.; Liable-Sands, L. M.; Incarvito, C.; Rheingold, A. L.; Stern, C. L. *Organometallics* **1999**, *18*, 4856−4868.
(14) Dixon, F. M.; Eisenberg, A. H.; Farrell, J. R.; Mirkin, C. A.; Liable-Sands, L. M.; Rheingold, A. L. *Inorg. Chem.* **2000**, *39*, 3432−3433.
(15) Singewald, E. T.; Mirkin, C. A.; Levy, A. D.; Stern, C. L. *Angew. Chem., Int. Ed. Engl.* **1994**, *33*, 2473−2475.
(16) Singewald, E. T.; Shi, X.; Mirkin, C. A.; Schofer, S. J.; Stern, C. L. *Organometallics* **1996**, *15*, 3062−3069.
(17) Singewald, E. T.; Slone, C. S.; Stern, C. L.; Mirkin, C. A.; Yap, G. P. A.; Liable-Sands, L. M.; Rheingold, A. L. *J. Am. Chem. Soc.* **1997**, *119*, 3048−3056.
(18) Slone, C. S.; Mirkin, C. A.; Yap, G. P. A.; Guzei, I. A.; Rheingold, A. L. *J. Am. Chem. Soc.* **1997**, *119*, 10743−10753.
(19) Allgeier, A. M.; Singewald, E. T.; Mirkin, C. A.; Stern, C. L. *Organometallics* **1994**, *13*, 2928−2930.
(20) Allgeier, A. M.; Slone, C. S.; Mirkin, C. A.; Liable-Sands, L. M.; Yap, G. P. A.; Rheingold, A. L. *J. Am. Chem. Soc.* **1997**, *119*, 550−559.
(21) Higgins, T. B.; Mirkin, C. A. *Inorg. Chim. Acta* **1995**, *240*, 347−353.
(22) Slone, C. S.; Weinberger, D. A.; Mirkin, C. A. In *Progress In Inorganic Chemistry*; Karlin, K. D., Ed.; John Wiley & Sons: New York, 1999; Vol. 48, pp 233−350.
(23) Bader, A.; Lindner, E. *Coord. Chem. Rev.* **1991**, *108*, 27−110.
(24) Lindner, E.; Pautz, S.; Haustein, M. *Coord. Chem. Rev.* **1996**, *155*, 145−162.

10.1021/om001042z CCC: $20.00
Publication on Web 04/07/2001

Scheme 1

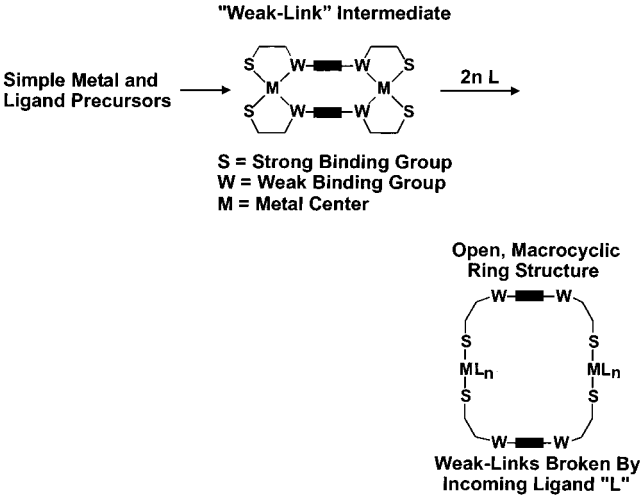

Scheme 2

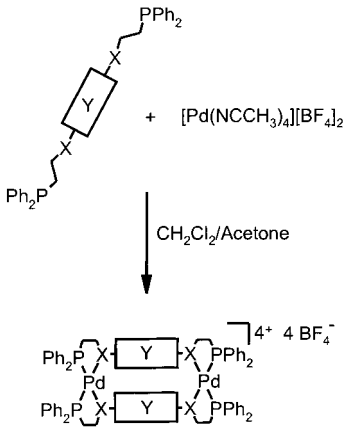

4: X=O, Y=1,4-$C_6(CH_3)_4$
5: X=O, Y=1,4-C_6H_4
6: X=S, Y=1,4-C_6H_4

units are used in the weak-link synthetic strategy. Reaction of such ligands with an appropriate metal starting material yields bimetallic condensed intermediates (shown in Scheme 1) that contain (1) strong metal−phosphorus bonds, (2) weak ether−metal, thioether−metal, or η^6-arene−metal bonds, and (3) thermodynamically stable five- and six-membered rings. These intermediates often can be isolated in near quantitative yield (vide infra) or used to form macrocycles by introducing them to ligands that can break their weak metal−heteroatom or metal− η^6-arene links (Scheme 1). Alternatively, the condensed intermediates can be used to construct more complex three-dimensional architectures. For example, three-tiered macrocycles containing guest molecules spanning the two macrocyclic metal centers are constructed by reacting small bifunctional aromatic molecules with the condensed structures to break their weak links.[10,12] In addition, molecular cylinders containing ligands bound between the metal sites of two macrocycles can be synthesized when large bifunctional aromatic molecules are added to the condensed structures.[11] Indeed, it is the flexibility of the ligands used and the coordinative unsaturation or lability of the metal centers generated in the complexes formed via the weak-link approach that, in part, differentiate this approach from other approaches to synthesizing supramolecular architectures.

Although the generality of the weak-link methodology has been demonstrated with respect to several types of hemilabile ligands, the utility of the synthetic approach has yet to be demonstrated with transition metals other than Rh(I). Ligand tailorability has allowed us to control macrocycle size, the hydrophobicity and photophysical properties of the macrocycle cavities, the complexing properties of the organic portion of the macrocycles, and the steric and electronic environments of the transition metals that comprise the macrocycles. Expanding the types of transition metals that can be utilized in the weak-link approach would provide increased tailorability with regard to the small molecule binding and catalytic properties of the resulting macrocycles. Herein, we demonstrate how the weak-link approach can be used to construct a variety of neutral and tetracationic 26-membered macrocycle rings with two Pd(II) metal centers.

Experimental Section

General Procedures. Unless otherwise noted, all reactions and manipulations were performed under a dry, inert atmosphere of nitrogen using standard Schlenk techniques. Acetone was distilled over K_2CO_3, THF and diethyl ether were doubly distilled over Na/benzophenone, and CH_2Cl_2 was distilled over NaH. All the solvents were bubbled with nitrogen before use. The deuterated solvents were purchased and used as received from Cambridge Isotopes Laboratories. The ligands 1,4-(PPh_2-$CH_2CH_2Y)_2R$ (**1**, Y = O, R = 2,3,5,6-$(CH_3)C_6$, and **3**, Y = S, R = C_6H_4) were prepared as previously reported.[13,14] Compound **2** (Y = O, R = C_6H_4) was synthesized from a new precursor (vide infra) as previously reported.[13]

Physical Measurements. $^{31}P\{^1H\}$ NMR spectra were recorded on a Varian 300 MHz Gemini or Mercury spectrometer and referenced versus an external 85% H_3PO_4 standard. The ^1H NMR spectra were obtained using a Varian 300 MHz spectrometer and referenced relative to residual proton resonance in deuterated solvents. Electrospray mass spectrometry (ESMS) for compounds **6** and **11** was performed on a Micromass Quatro II electrospray triple quadropole mass spectrometer. ESMS for compounds **7**−**10** was obtained with a Micromass Quattro I quadrupole-hexapole-quadrupole (QHQ) mass spectrometer. The electron ionization mass spectrometry (EIMS) was performed on a Fisions VG 70-250 SE mass spectrometer. Melting point temperatures were recorded on a Mel-Temp II melting temperature apparatus (Laboratory Devices of Holliston, MA). Elemental analysis were obtained from Quantitative Technologies Inc. of Whitehouse, NJ.

Synthesis of 1,4-((p-$CH_3C_6H_4SO_3$)$(CH_2CH_2O))_2C_6H_4$, a Precursor for 2. Bis(2-hydroxyethyl)ether hydroquinone (5.0 g, 0.025 mol) was added to a 300 mL Schlenk flask fitted with an addition funnel. The solid was suspended in CH_2Cl_2 (150 mL) and stirred for 30 min followed by the addition of $(CH_3CH_2)_3N$ (10 mL, 0.7765 g/mL, 0.077 mol). The solution was cooled with an external ice bath. The addition funnel was subsequently charged with a tosyl chloride solution (14.4 g, 0.076 mol, 1.52 M) in CH_2Cl_2, which was added dropwise over 30 min to the hydroquinone solution while stirring. After the addition was complete, the ice bath was removed to allow the reaction to warm to room temperature. After stirring overnight (12 h), the organic fraction was washed with two portions of water (50 mL each), made acidic (pH 5) with dilute HCl, neutralized with saturated aqueous $NaHCO_3$, and then dried over $MgSO_4$. The resulting product was washed with diethyl ether to remove the excess tosyl chloride and yield a spectroscopically pure white solid. Isolated yield = 11.3 g, 0.022 mol,

88%. ^{1}H NMR: ($CDCl_3$) δ 7.82 (d, 4H, *p*-$CH_3C_6H_4SO_3$, J_{H-H} = 8.28 Hz), 7.35 (d, 4H, *p*-$CH_3C_6H_4SO_3$, J_{H-H} = 8.07 Hz), 6.70 (s, 4H, C_6H_4), 4.33 (t, 4H, CH_2, J_{H-H} = 4.78 Hz), 4.09 (t, 4H, CH_2, J_{H-H} = 4.74 Hz), 2.46 (s, 6H, *p*-$CH_3C_6H_4SO_3$). ^{13}C NMR: (CD_3Cl) δ 152.82, 145.17, 132.98, 129.98, 128.06, 115.84, 68.41, 66.32, 21.95. EIMS: $[M]^+$ calcd 506.10682, found 506.10673 *m*/*z*. Mp: 146−147 °C. $C_{24}H_{26}O_8S_2 \cdot 0.5\ H_2O$: calcd 55.91% C, 5.28% H, found 55.92% C, 5.23% H.

General Syntheses of Complexes [(μ-(1,4-($PPh_2CH_2CH_2O$)$_2$-2,3,5,6-((CH_3)$_4C_6$))$_2$$Pd_2$)][$BF_4$]$_4$ (4) and [(μ-(1,4-($PPh_2CH_2CH_2O$)$_2C_6H_4$))$_2$$Pd_2$)][$BF_4$]$_4$ (5). A 100 mL CH_2Cl_2 solution of **1** or **2** (0.050 or 0.060 g, 0.086 or 0.112 mmol, respectively) was added over 1 h to a stirred 100 mL acetone solution of $[Pd(NCCH_3)_4][BF_4]_2$ (0.038 or 0.050 g, 0.086 or 0.112 mmol, respectively) while cooling the reaction mixture to −40 °C in a N_2/acetone bath. The resulting mixture was stirred for 6 h at room temperature to yield a yellow-orange solution. The solvent was removed in vacuo to yield yellow-orange powders of **4** and a mixture of products containing **5**,[25] respectively.

[(μ-(1,4-($PPh_2CH_2CH_2O$)$_2$-2,3,5,6-((CH_3)$_4C_6$))$_2$$Pd_2$)][$BF_4$]$_4$ (4). Complex **4** formed in quantitative yield as characterized by ^{31}P{^{1}H} and ^{1}H NMR spectroscopies. Isolated yield: 93.9%. ^{31}P{^{1}H} NMR: (CD_3NO_2) δ 61.4 (s). ^{1}H NMR: (CD_3NO_2) δ 7.74 (m, 16H, P(C_6H_5)$_2$), 7.59 (m, 12H, P(C_6H_5)$_2$), 4.12 (m, 8H, CH_2), 3.54 (br, 8H, CH_2), 2.35 (s, 12H, CH_3). Dec pt: 200−201 °C. $C_{76}H_{80}O_4P_4Pd_2B_4F_{16} \cdot 0.5\ CD_3NO_2$: calcd 51.81% C, 4.72% H, 0.39% N, found 51.67% C, 5.08% H, 0.15% N. The nitromethane found in the combustion analysis is from the NMR solvent and is seen in the crystal structure of the analogous compound, **6**.

Synthesis of [(μ-(1,4-($PPh_2CH_2CH_2S$)$_2C_6H_4$))$_2$$Pd_2$)][$BF_4$]$_4$ (6). A 10 mL CH_2Cl_2 solution of **3** (0.053 g, 0.113 mmol) was added over 15 min to a stirred 15 mL acetone solution of $[Pd(NCCH_3)_4][BF_4]_2$ (0.049 g, 0.111 mmol) in a glovebox. The resulting mixture was stirred overnight at room temperature to yield an orange solution with an orange precipitate. The solvent was removed in vacuo to yield an orange powder. Complex **6** formed in quantitative yield as determined by ^{31}P{^{1}H} and ^{1}H NMR spectroscopies. ^{31}P{^{1}H} NMR: (CD_3NO_2) δ 68.9 (s). ^{1}H NMR: (CD_3NO_2) δ 7.6 (m, 16H, P(C_6H_5)$_2$), 7.5 (m, 16H, P(C_6H_5)$_2$),7.3 (s, 8H, P(C_6H_5)$_2$) 3.4 (br, 8H, CH_2), 3.3 (br, 8H, CH_2). ESMS: $[[M]^{4+}[BF_4]_3^-]^+$ calcd 1606.6, found 1606.3 *m*/*z*. $[[M]^{4+}[BF_4]^-]^{3+}$: calcd 477.7, found 477.7 *m*/*z*. Dec pt: 236 °C. $C_{68}H_{64}S_4P_4Pd_2B_4F_{16}$: calcd 48.23% C, 3.81% H, 0% N, found 47.89% C, 3.98% H, 0.16% N.

General Procedure for the Synthesis of [(μ-(1,4-(PPh_2-CH_2CH_2O)$_2$-2,3,5,6-((CH_3)$_4C_6$))$_2$(CH_3CN)$_4$$Pd_2$)][$BF_4$]$_4$ (7) and [(μ-(1,4-($PPh_2CH_2CH_2O$)$_2C_6H_4$))$_2$(CH_3CN)$_4$$Pd_2$)][$BF_4$]$_4$ (8). Complex **4** or mixture **5** (10 mg) was dissolved in 1 mL of CH_3CN to yield **7** or **8**. To obtain NMR spectra, the solvent was removed in vacuo, and the product was then redissolved in 1 mL of CD_3CN to yield a yellow solution of **7** or **8** in quantitative yield as determined by ^{31}P{^{1}H} and ^{1}H NMR spectroscopies.

[(μ^2-(1,4-($PPh_2CH_2CH_2O$)$_2$-2,3,5,6-((CH_3)$_4C_6$))$_2$(CH_3CN)$_4$-Pd_2)][BF_4]$_4$ (7). ^{31}P{^{1}H} NMR: (CD_3CN) δ 25.7 (s). ^{1}H NMR: (CD_3CN) δ 7.65 (m, 22 H, P(C_6H_5)$_2$), 7.50 (m, 18H, P(C_6H_5)$_2$), 4.25 (br, 8H, CH_2), 2.79 (br, 8H, CH_2), 2.24 (s, 12H, CH_3). ESMS: $[[M]^{4+}$ − 4 $CH_3CN]^{4+}$ calcd 348.6, found 348.6 *m*/*z*. $C_{84}H_{92}O_4P_4Pd_2N_4B_4F_{16} \cdot 2CH_3CN$: calcd 53.17% C, 4.97% H, 4.23% N, found 53.63% C, 5.08% H, 4.09% N. The excess acetonitrile found in the combustion analysis is a result of sample preparation. The lability of acetonitrile ligands prohibits complete drying in vacuo and results in residual solvent being present.

(25) **5:** ESMS: $[[M]^{4+}[BF_4]^{3-}]^+$ calcd 1541.2, found 1542.2 *m*/*z*. $[M]^{4+}$ calcd 320.05, found 320.3 *m*/*z*. $C_{68}H_{64}O_4P_4Pd_2B_4F_{16} \cdot CD_3NO_2$: calcd 48.94% C, 4.16% H, 0.83% N, found 49.12% C, 4.23% H, 0.90% N. The nitromethane found in the combustion analysis is from the NMR solvent and is seen in the crystal structure of the analogous compound, **6**.

Chart 1

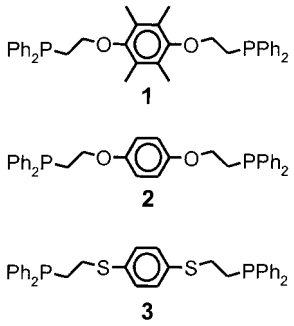

[(μ-(1,4-($PPh_2CH_2CH_2O$)$_2C_6H_4$))$_2$(CH_3CN)$_4$$Pd_2$)][$BF_4$]$_4$ (8). Crystallization of **8** by layering a solution of CD_3CN and CD_3NO_2 with pentane afforded yellow blocks, suitable for a single-crystal X-ray diffraction study. ^{31}P{^{1}H} NMR: (CD_3CN) δ 28.6 (s). ^{1}H NMR: (CD_3CN) δ 7.7−7.3 (m, 16H, P(C_6H_5)$_2$), 6.87 (s, 8H, C_6H_4), 4.50 (m, 8H, CH_2), 2.85 (s, 8H, CH_2). ESMS: $[[M]^{4+}$ − 4 $CH_3CN]^{4+}$ calcd 320.5, expt 320.7 *m*/*z*. $C_{76}H_{76}O_4P_4Pd_2N_4B_4F_{16}$: calcd 50.90% C, 4.27% H, 3.12% N, found 51.46% C, 4.38% H, 2.92% N.

General Procedure for the Synthesis of [(μ-(1,4-($PPh_2CH_2CH_2O$)$_2$-2,3,5,6-((CH_3)$_4C_6$))$_2$(CN)$_4$$Pd_2$)] (9), [($\mu$-(1,4-($PPh_2CH_2CH_2O$)$_2C_6H_4$))$_2$($CN$)$_4$$Pd_2$)] (10), and [($\mu$-(1,4-($PPh_2CH_2CH_2S$)$_2C_6H_4$))$_2$($CN$)$_4$$Pd_2$)] (11). Complex **4**, mixture **5**, or **6** (10 mg) was suspended in CD_3OD. To this, 4 equiv of a solution of KCN in CD_3OD was added (0.098 M). Upon mixing, a white precipitate formed, which was isolated by filtering the mixture through Celite. The solid was redissolved in CD_2Cl_2 to yield **9**, **10**, or **11** in quantitative yield as determined by ^{31}P{^{1}H} and ^{1}H NMR spectroscopies.

[(μ-(1,4-($PPh_2CH_2CH_2O$)$_2$-2,3,5,6-((CH_3)$_4C_6$))$_2$(CN)$_4$-Pd_2)] (9). Crystallization of **9** by layering a solution of CD_2Cl_2 with pentane yielded yellow needles suitable for a single-crystal X-ray diffraction study. ^{31}P{^{1}H} NMR: (CD_2Cl_2) δ 18.3 (s). ^{1}H NMR: (CD_2Cl_2) δ 7.69 (m, 16H, P(C_6H_5)$_2$), 7.50 (m, 8H, P(C_6H_5)$_2$), 7.40 (m, 16H, P(C_6H_5)$_2$), 3.94 (m, 8H, CH_2), 3.18 (m, 8H, CH_2), 1.92 (s, 24H, CH_3). ESMS: $[M-CN]^+$ calcd 1472.2, found 1472.2 *m*/*z*.

[(μ-(1,4-($PPh_2CH_2CH_2O$)$_2C_6H_4$))$_2$(CN)$_4$$Pd_2$)] (10). ^{31}P{^{1}H} NMR: (CD_3NO_2) δ 17.9 (s). ^{1}H NMR: (CD_3NO_2) δ 7.64 (m, 16H, P(C_6H_5)$_2$), 7.46 (m, 8H, P(C_6H_5)$_2$), 7.41 (m, 16H, P(C_6H_5)$_2$), 6.67 (s, 8H, C_6H_4), 4.28 (br, 8H, CH_2), 3.14 (br, 8H, CH_2). ESMS: $[M - CN]^+$ calcd 1360.0, found 1359.1 *m*/*z*.

[(μ-(1,4-($PPh_2CH_2CH_2S$)$_2C_6H_4$))$_2$(CN)$_4$$Pd_2$)] (11). ^{31}P{^{1}H} NMR: (CD_3NO_2) δ 17.1 (s). ^{1}H NMR: (CD_3NO_2) δ 8.60 (m, 22 H, P(C_6H_5)$_2$), 8.45 (m, 18H, P(C_6H_5)$_2$), 4.06 (br, 8H, SCH_2), 3.79 (br, 8H, PCH_2). ESMS: $[M - CN]^+$ calcd 1424.28, found 1424.4 *m*/*z*.

Results

Ligands 1−3. The three ligands used in this study (Chart 1) were synthesized either by methodologies reported in the Experimental Section or elsewhere from their respective quinone or hydroquinone precursors.[13,14] All of the ligands are moderately air-sensitive white solids and have been characterized by ^{1}H and ^{31}P{^{1}H} NMR spectroscopies, mass spectrometry, and melting-point analysis.

Synthesis and Characterization of the Condensed Macrocycles, 4−6. The palladium condensed intermediates **4**−**6** were synthesized via a route similar to the one used to prepare the analogous rhodium macrocycles (Scheme 2).[10−14] Ligands **1** and **3**, dissolved in CH_2Cl_2, were reacted with $[Pd(CH_3CN)_4][BF_4]_2$ to form **4** and **6**, respectively. In this reaction, the labile

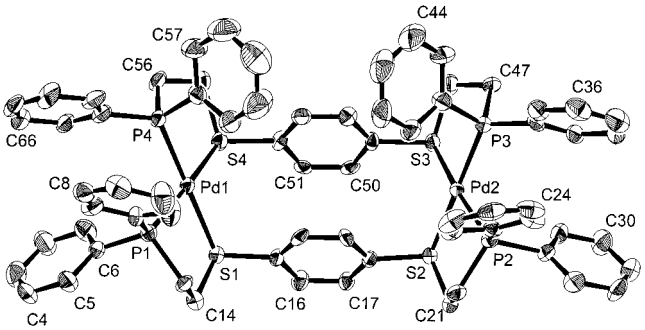

Figure 1. ORTEP diagram of **6**·3CD_3NO_2 showing atom-labeling scheme. Unlabeled atoms follow the same numbering scheme as labeled atoms. Thermal ellipsoids are shown at 30% probability, and hydrogen atoms, counterions, and solvent molecules are omitted for clarity.

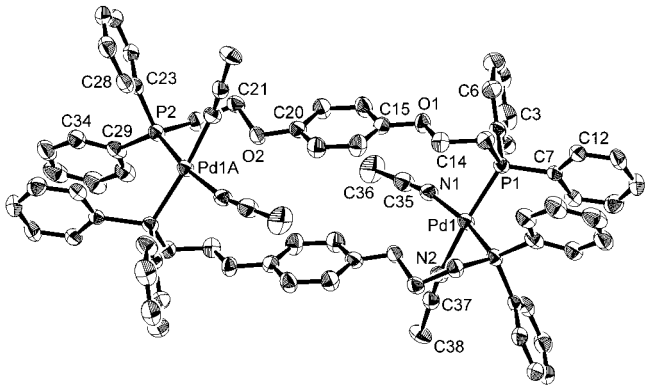

Figure 2. ORTEP diagram of **8**·CH_3CN·2CH_3NO_2 showing atom-labeling scheme. Unlabeled atoms follow the same numbering scheme as labeled atoms. Thermal ellipsoids are shown at 50% probability, and hydrogen atoms, counterions, and solvent molecules are omitted for clarity.

acetonitrile ligands are displaced by the stronger binding P, O, and S atoms of ligands **1** and **3** to produce the corresponding condensed intermediates **4** and **6** in high yield (>94%). Ligand **2** also reacts with $[Pd(CH_3CN)_4][BF_4]_2$ under comparable conditions, but forms a mixture of several products, one of which has been spectroscopically identified as condensed intermediate **5**. No attempts were made to isolate **5** from the mixture since all species can be converted to the same macrocycle via reaction with acetonitrile (vide supra).

The $^{31}P\{^1H\}$ NMR spectra of **4**−**6** are very diagnostic of their structures and compare well with literature values for isoelectronic and isostructural complexes formed from Rh. Ether-containing compounds **4** and **5** exhibit characteristic resonances at δ 61.4 and δ 59.2, respectively, which compare well with the chemical shift for a related Rh(I) analogue of these complexes (δ 61.4).[13,26] Thioether-containing complex **6** was fully characterized in solution and in the solid state, and all data are consistent with the solid-state structure determined by single-crystal X-ray diffraction (Scheme 2 and Figure 1).

Solid-State Characterization of 6. The structure of **6**·3CD_3NO_2 was determined by single-crystal X-ray diffraction methods (Figure 1). The coordination environment around the Pd atom is distorted square planar, and the intermolecular bond and nonbonded distances compare well with the analogous Rh complex that has recently been reported.[14] The average Pd−P and Pd−S distances are 2.298 and 2.402 Å, respectively, compared to the Rh−P and Rh−S average distances of 2.253 and 2.350 Å, respectively, in the Rh analogue of **6**. The Pd−Pd distance is 8.003 Å, and the arene−arene distance is 3.531 Å, on the order of $\pi-\pi$ stacking interactions. For the rhodium analogue, the Rh−Rh distance is 8.381, and the arene−arene distance is 3.51 Å. Unlike the rhodium analogue, structure **6** folds, slightly, at the sulfur atoms. The fold is due to the distorted, yet characteristic, tetrahedral sulfur bonding environment.[27] As a result, all of the phenyl groups on the phosphorus atoms point out of one face of the molecule.

Synthesis and Characterization of the Tetraacetonitrile Adducts of 7 and 8. A defining characteristic of our weak-link approach is the ability to break the weak metal−heteroatom links in the condensed intermediates with stronger binding π-acceptors or σ-donors to form macrocyclic structures. In the case of **4** and **5**, this can be effected by dissolving **4** or the mixture containing **5** in CH_3CN (Scheme 3). The $^{31}P\{^1H\}$ NMR spectra of the resulting products, **7** and **8**, each exhibit a single resonance at 25.7 and 28.6 ppm, respectively. This complete and upfield shift is consistent with macrocycle formation. Significantly, although these complexes were both formed in a two-step process where the intermediates were isolated, they also can be synthesized in a simple one-step process by adding excess acetonitrile to the crude reaction mixtures.[28]

Solid-State Characterization of 8. The solid-state structure of **8**·CH_3CN·CH_3NO_2 was determined by a single-crystal X-ray diffraction study, and an ORTEP diagram is shown in Figure 2. Crystallographic data are shown in Table 1, and selected bond lengths and angles are given in Table 2. With the exception of the disordered solvent molecules and one BF_4^- anion, all other non-hydrogen atoms were refined anisotropically. The BF_4^- anion that was not refined anisotropically was found in the difference map and was set as two rigid groups of differing occupancies. The group's isotropic thermal parameters were refined, but the positions were not. The CH_3NO_2 molecule that lies outside the cavity of the macrocycle had occupancies of 0.333 and 0.667 assigned to the carbon and oxygen atoms, respectively. The sets of carbon and oxygen atoms were constrained to the same positions, and hydrogen atoms were not included on this disordered solvent molecule. Each of the Pd atoms has adopted a distorted square planar coordination geometry. The average Pd−P bond length ($Pd-P_{av}$ = 2.27 Å) and Pd−N bond length ($Pd-N_{av}$ = 2.09 Å) are similar to the acetonitrile-containing rhodium analogues constructed from ligand **1** ($Rh-P_{av}$ = 2.33 Å, $Rh-N_{av}$ = 2.07 Å).[13] The Pd−Pd distance is 9.78 Å, and the distance between the arene centroids is 4.63 Å. The plane of carbons of the center benzene ring (C15−C20) has an average out-of-plane distance of 0.012 Å. The acetonitrile molecules are bound *cis* to one another, and the plane defined by Pd1, N1, and N2 has

(26) The related Rh complex is isostructural.
(27) Murray, S. G.; Hartley, F. R. *Chem. Rev.* **1981**, *81*, 365−414.
(28) In a two-step process, the first reaction yields an intermediate that is isolated to use in the second reaction to yield the final product. In a one-step process, the intermediate is not isolated but, instead, reacted in situ to yield the desired final product.

Scheme 3

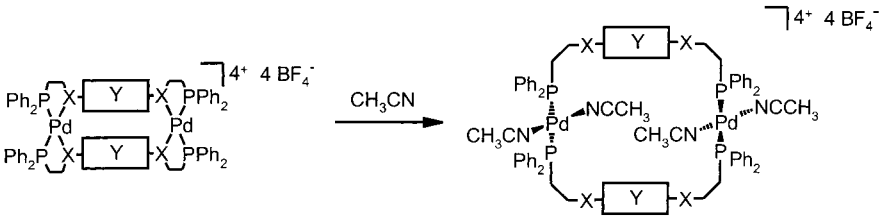

7: X=O, Y=1,4-$C_6(CH_3)_4$
8: X=O, Y=1,4-C_6H_4

Table 1. Crystallographic Data

	6·3CD_3NO_2	**8**·CH_3CN·2CH_3NO_2	**9**
formula	$C_{71}H_{64}B_4D_9F_{16}N_3O_6P_4Pd_2$	$C_{80}H_{82}P_4O_8Pd_2B_4F_{16}N_7$	$C_{82}O_4H_{84}N_4Pd_2Cl_4$
fw	1885.54	1953.48	1668.10
color, habit	orange plate	yellow, cut plate	colorless, needle
cryst dimens (mm)	0.25 × 0.20 × 0.15	0.12 × 0.21 × 0.20	0.06 × 0.06 × 0.48
temp (K)	173(2)	153(1)	153(1)
cryst syst	triclinic	triclinic	monoclinic
a (Å)	15.8113(2)	10.2299(6)	8.958(2)
b (Å)	16.1369(2)	12.1537(7)	19.385(4)
c (Å)	17.1565(2)	17.4449(10)	22.366(5)
α (deg)	90.4108(9)	81.7050(9)	
β (deg)	103.7363(7)	82.436(10)	100.8366(5)
γ (deg)	109.1194(5)	89.5600(9)	
V (Å^3)	4000.41(7)	2127.4(2)	3814.7(13)
space group	$P\bar{1}$	$P\bar{1}$	$P2_1/n$
Z	2	1	2
μ (cm^{-1})	7.23 (Mo Kα)	5.91 (Mo Kα)	7.49 (Mo Kα)
$2\theta_{max}$ (deg)	48.0	56.6	56.6
diffractometer	Siemens P4/CCD	SMART-1000 CCD	SMART-1000 CCD
X-radiation (*λ*, Å)	Mo Kα (0.71073), graphite monochromated	Mo Kα (0.71073), graphite monochromated	Mo Kα (0.71073), graphite monochromated
total no. of reflns	25 267	19 533	35 064
no. of unique reflns	11 889	9853	9127
no. of variables	883	462	246
R_{int}	0.0469	0.021	0.297
corrections (transmn factors)	SADABS (0.956−0.888)	SADABS, Bruker (1.000−0.919)	XPREP, SHELXTL (0.973−0.855)
R1, wR2[a]	0.0741, 0.1934	0.067, 0.215	0.063, 0.147
residual ρ (e Å^{-3})	+1.083, −0.592	2.10, −1.20	+1.8, −0.71
GOF	1.438	1.09	0.98

[a] $R1 = \Sigma||F_o| - |F_c||/\Sigma|F_o|$, $wR2 = [\Sigma(w(F_o^2 - F_c^2)^2)/\Sigma w(F_o^2)^2]^{1/2}$, $w = 1/\sigma^2(F^2)$.

Scheme 4

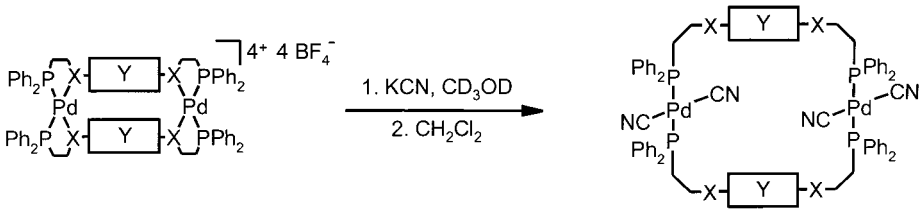

9: X=O, Y=1,4-$C_6(CH_3)_4$
10: X=O, Y=1,4-C_6H_4
11: X=S, Y=1,4-C_6H_4

a dihedral angle of 144.73° with respect to the plane defined by the benzene ring comprised of C15−C20. The *cis*-geometry is due, most likely, to the strong *trans*-directing properties of the phosphines.[29]

Synthesis and Characterization of Neutral, CN Macrocycles 9, 10, and 11. The neutral, tetracyanide complexes **9**, **10**, and **11** were synthesized by adding 4 equiv of KCN to a CD_3OD suspension of **4**, the mixture containing **5**, and **6**, respectively (Scheme 4). One product formed in each reaction, as evidenced by a singlet at δ 18.3, 17.9, and 17.1 in the respective $^{31}P\{^1H\}$ NMR spectra. These shifts compare well with those measured for related mononuclear and binuclear palladium(II) bis(diphenylphosphino)methane complexes (δ 16.9 and 11.4).[30,31] It is important to note that the cyanide ligands form exceptionally strong bonds to the Pd centers. Indeed, when an excess of KCN is added to

(29) Amabilino, D. B.; Stoddart, J. F. *Chem. Rev.* **1995**, *95*, 2725−2828.

(30) Hassan, F. S. M.; Markhan, D. P.; Pringle, P. G.; Shaw, B. L. *J. Chem. Soc., Dalton Trans.* **1985**, 279−283.

(31) Pringle, P. G.; Shaw, B. L. *J. Chem. Soc., Chem. Commun.* **1982**, 956−957.

Table 2. Selected Bond Distances and Angles

	bond distances (Å)		bond angles (deg)	
6·3CD_3NO_2	Pd1−Pd2	8.003	P1−Pd1−P4	97.21(7)
	arene−arene	3.531	P4−Pd1−S4	85.24(7)
	Pd1−S1	2.4062(19)	P1−Pd1−S4	171.71(8)
	Pd1−S4	2.365(2)	P4−Pd1−S1	176.81(8)
	Pd1−P1	2.298(2)	P1−Pd1−S1	85.07(7)
	Pd1−P4	2.296(2)	S4−Pd1−S1	92.20(7)
8·CH_3CN·2CH_3NO_2	Pd1−P1	2.259(2)	P1−Pd1−P2	94.57(7)
	Pd1−P2	2.277(2)	P1−Pd1−N1	92.5(2)
	Pd1−N1	2.091(6)	P1−Pd1−N2	170.0(2)
	Pd1−N2	2.096(6)	P2−Pd1−N1	168.7(2)
	Pd1−Pd1A	9.78	P2−Pd1−N2	89.2(2)
	arene−arene	4.63	N1−Pd1−N2	85.3(2)
	N1−C35	1.140(9)	Pd1−N1−C35	167.8(7)
	N2−C37	1.127(9)	Pd1−N2−C37	160.1(6)
9	Pd1−P1	2.324(3)	P1−Pd1−P2	166.53(9)
	Pd1−P2	2.329(3)	P1−Pd1−C1	86.1(3)
	Pd1−C1	2.055(9)	P1−Pd1−C2	94.2(3)
	Pd1−C2	2.028(10)	P2−Pd1−C1	91.0(3)
	Pd1−Pd1A	10.99	P2−Pd1−C2	88.2(3)
	arene−arene	6.99	C1−Pd1−C2	177.4(4)
	C1−N1	1.067(11)	Pd1−C1−N1	173.1(11)
	C2−N2	1.085(12)	Pd1−C2−N2	176.9(10)

4 or **6**, the phosphinoalkyletheraryl and phosphinoalkylthioetheraryl ligands are completely displaced from the Pd center, as evidenced by $^{31}P\{^1H\}$ NMR spectroscopy.

Solid-State Characterization of 9. The solid-state structure of **9** has been determined by a single-crystal X-ray diffraction study, and an ORTEP diagram is shown in Figure 3. Crystallographic data are shown in Table 1, and selected bond lengths and angles are given in Table 2. Owing to the paucity of data, only the noncarbon atoms were refined anisotropically. The coordination geometry around each of the Pd atoms is distorted square planar, and the cyanide groups are clearly trans to one another. The Pd−Pd distance is 10.99 Å, and the distance between the arene−arene centroids is 6.99 Å. These distances are similar to the rhodium complex constructed from ligand **1** after the weak links were broken though the addition of CO and CH_3CN (Rh−Rh = 11.61 and arene−arene = 6.44 Å).[13] The average Pd−P distances (2.33 Å) are similar to the Rh−P distances (2.32 Å) for the neutral rhodium macrocycle synthesized from ligand **2**, $[(CH_3)_4N]Cl$, and CO.[14] The average distance out of the plane defined by C17−C22 is 0.005 Å, and 0.018 Å for the plane defined by C17−C26. The dihedral angle of the plane defined by C17−C22 versus that of Pd1, C1, and C2 is 84.99°.

Discussion

The Pd metallomacrocycles reported herein provide a basis for comparison with their Rh(I) analogues. Both Rh(I) and Pd(II) are d^8 transition metals, favor square planar geometries, and often exhibit similar chemistries. However, the common chelating environments around the Pd and Rh metal centers are somewhat different. Notably, Rh(I) can accommodate an 18-electron configuration via η^6-arene coordination of the hemilabile ligand; therefore, "slipped macrocycles" such as **13** are often observed for reactions that utilize hemilabile ligands and involve Rh(I) (Scheme 5). This is especially true for hemilabile ligands that have extraordinarily weakly binding heteroatoms, such as ligand **1**, where the arene can form a stronger interaction with the metal center than the ether moieties. It is important to note

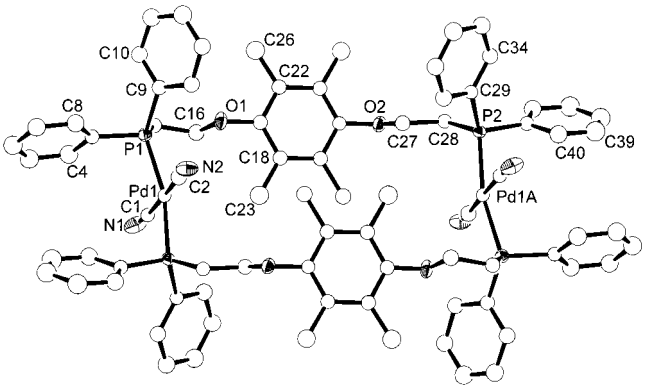

Figure 3. ORTEP diagram of **9** showing atom-labeling scheme. Unlabeled atoms follow the same numbering scheme as labeled atoms. Thermal ellipsoids are shown at 50% probability, and hydrogen atoms are omitted for clarity.

Scheme 5

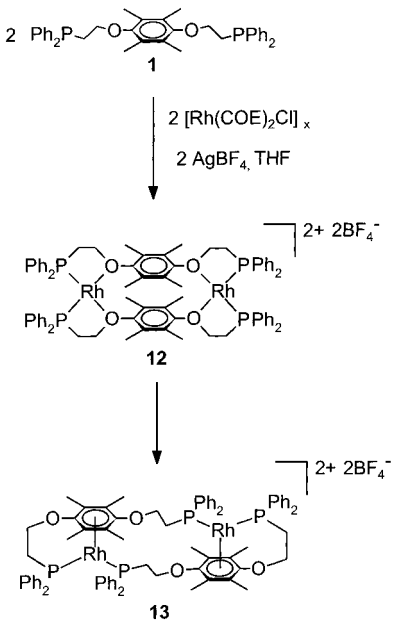

that even in the case of Rh(I), where the "slipped intermediate forms", it has been shown that the "bow tie" structure is the kinetic product and the slipped intermediate is the local thermodynamic minimum (Scheme 5).[13] Hence, the weakly binding O atoms are important for bonding to the metal centers and directing the formation of the binuclear closed macrocycle. In contrast, η^6-arene bonding is not a common mode for bis-phosphine Pd(II) fragments. Consequently, in the case of intermediate **5**, which derives from ligand **2**, the "bow tie" structure forms but quickly establishes an equilibrium with the remaining equivalents of acetonitrile to form a series of partially opened products. Significantly, the equilibrium can be driven to the open macrocycle product, **8**, in quantitative fashion simply by adding more acetonitrile to the mixture of compounds. Note that for ligands **1** and **3**, which have more strongly binding ether and thioether groups, respectively, the "bow tie" condensed intermediates **4** and **6** are formed in quantitative yield. The relative stability of **4** as compared with **5** is enhanced by the more basic ether atoms in **1** as compared with **2** and the greater π-stacking and van der Waals interactions associated

with durenyl groups in **4** as compared with the proton-substituted arenes in **5**.

In the case of ligand **3** and Pd(II), the clean formation of the bow tie intermediate **6** is easy to understand. The strong binding of the P and S atoms in ligand **3** to Pd centers directs the formation of intermediate **6**. As with Rh(I), acetonitrile is not sufficient to break the metal−S links in **6** to form an open macrocycle. However, strongly binding CN^- ligands can be employed to cleanly break these links and form an open macrocyclic structure **11**. This novel CN^--induced opening of condensed intermediates has been extended to the Pd systems with weakly bound ether atoms as well, providing a general route to open neutral metallomacrocycles with four-coordinated cyanide moieties.

Conclusions

Herein, we have shown that the weak-link approach can be extended beyond Rh(I) to Pd(II). By using hemilabile ligands to template the formation of condensed intermediates, both cationic and neutral macrocycles have been synthesized in high yield from simple ligand and metal precursors. The weak-link routes to Pd(II) and Rh(I) metallomacrocycles are similar, but exhibit some notably different characteristics. In particular, Rh(I) can accommodate η^6-arene interactions, which leads to intermediates that are not observed in the case of Pd(II). Regardless, the basic principle of the weak-link approach stands for both metals: a hemilabile ligand with proper chelate size can template the formation of a binuclear intermediate that can be subsequently opened into a macrocycle in high yield. The extension of this approach to Pd(II) should open new avenues to binuclear catalysts with activities and selectivities that can be tailored by virtue of the size, shape, and ancillary ligands that comprise the macrocycles generated via this approach.

Acknowledgment. C.A.M. acknowledges the Georgia Institute of Technology Molecular Design Institute under ONR Contract No. G-29-X03-G6/N000 14-95-1-111 and NSF (CHE-9625391) for support of this research. F.M.D. acknowledges the Illinois Minority Graduate Incentive Program for a predoctoral fellowship. Dr. Joshua Farrell and Dr. Igor Kourkine are acknowledged for helpful discussions. The Quattro I mass spectrometer at the University of Illinois was purchased in part with a grant from the Division of Research Resources, National Institutes of Health (RR 07141).

Supporting Information Available: Detailed X-ray structural data including a summary of crystallographic parameters, atomic coordinates, bond distances and angles, anisotropic thermal parameters, and H atom coordinates for **6**, **8**, and **9**. Sample ^{1}H NMR and ^{31}P {^{1}H} NMR spectra for **9**−**11**. This material is available free of charge via the Internet at http://pubs.acs.org.

OM001042Z